Available online at www.sciencedirect.com
ScienceDirect
Journal of Power Sources 160 (2006) 651–656
JOURNAL OF POWER SOURCES
www.elsevier.com/locate/jpowsour

# Improved electrochemical properties of a coin cell using $LiMn_{1.5}Ni_{0.5}O_4$ as cathode in the 5 V range

Rahul Singhal [a], Suprem R. Das [b], Osbert Oviedo [a], Maharaj S. Tomar [a], Ram S. Katiyar [b,*]

[a] *Department of Physics, University of Puerto Rico, Mayaguez, PR 00680-9016, USA*
[b] *Department of Physics, University of Puerto Rico, San Juan, PR 00931-3343, USA*

Received 22 January 2006; received in revised form 2 February 2006; accepted 3 February 2006
Available online 29 March 2006

**Abstract**

Phase pure $LiMn_{1.5}Ni_{0.5}O_4$ powders were synthesized by a chemical synthesis route and were subsequently characterized as cathode materials in a Li-ion coin cell comprising a Li anode and lithium hexafluorophosphate ($LiPF_6$), dissolved in dimethyl carbonate (DMC) + ethylene carbonate (EC) [1:1, v/v ratio] as electrolyte. The spinel structure and phase purity of the powders were characterized using X-ray diffraction and micro-Raman spectroscopy. The presence of both oxidation and reduction peaks in the cyclic voltammogram revealed $Li^+$ extraction and insertion from the spinel structure. The charge–discharge characteristics of the coin cell were performed in the 3.0–4.8 V range. An initial discharge capacity of $\sim$140 mAh $g^{-1}$ was obtained with 94% initial discharge capacity retention after 50 repeated cycles. The microstructures and compositions of the cathode before and after electrochemistry were investigated using scanning electron microscopy and energy-dispersive analysis by X-ray analysis, respectively. Using X-ray diffraction, Raman spectroscopy and electrochemical analysis, we correlated the structural stability and the electrochemical performance of this cathode.


*Keywords:* Li-ion battery; $LiMn_2O_4$; Spinel cathode; Discharge capacity

## 1. Introduction

Manganese based cathode materials such as $LiMn_2O_4$ (spinel structure) and $LiMnO_2$ (layered structure) are of vital research interest for Li-ion rechargeable battery applications because of they are less toxic and economically cheap [1–5]. Layered manganese cathodes have very good specific capacity but poor cyclability, probably because of the instabilities during electrochemical cycling, which can be attributed to several reasons [6,7]. Spinel $LiMn_2O_4$ has a reasonably good specific capacity (theoretical capacity 148 mAh $g^{-1}$) but it also problems of capacity fading and structural distortion from the cubic to tetragonal phase change while operating in the 3 V range [8–10] at elevated temperatures. However, the spinel $LiMn_2O_4$ has very good structural and electrochemical stability at room temperature and in the 4 V range of operation. Attempts are being made by various groups to understand the origin of the structural transformation and the phenomenon is mostly attributed to Jahn-Teller distortions [11–14]. Various cationic doping approaches are being used to overcome the problem and achieve improved performances [15–17]. One of the possible uses of $LiMn_2O_4$ is in the operation of electric vehicles, which require high energy density and operation at elevated temperatures and voltages. Sun et al. previously reported that at 55 °C, a pure $LiMn_{1.5}Ni_{0.5}O_4$ cathode undergoes severe capacity fading in the 5 V range of operation (capacity retention of no more than 10% after 30 cycles), but the capacity was retained up to almost the initial capacity of 137 mAh $g^{-1}$, after 50 repeated cycles when coated with ZnO. Further they also reported that ZnO coated $LiMn_{1.5}Ni_{0.5}O_4$ powder retains the cubic spinel structure after 50 cycles [18]. They obtained the discharge capacity for pure $LiMn_{1.5}Ni_{0.5}O_4$ at room temperatures, but no detailed characteristics at RT were given. Kanamura et al. reported a discharge capacity of 120 mAh $g^{-1}$ in the 5 V operation range of a coin cell using $LiMn_{1.5}Ni_{0.5}O_4$ cathode prepared by a solid-state

* Corresponding author. Tel.: +1 787 751 4210; fax: +1 787 764 2571.
*E-mail addresses:* rkatiyar@speclab.upr.edu, rkatiyar@hotmail.com (R.S. Katiyar).

0378-7753/$ – see front matter © 2006 Elsevier B.V. All rights reserved.
doi:10.1016/j.jpowsour.2006.02.021

reaction method using Ti and Al mesh current collectors, and according to them, the cell with a Ti-current collector showed degraded performance, while a cell with the Al current collector showed a better performance up to 30 discharge cycles [19]. Kobayashi et al. [20] reported a 5 V class of ceramic/polymer composite all-solid-state lithium battery with cell configuration of $Li_3PO_4$ coated $LiMn_{1.5}Ni_{0.5}O_4$ with solid polymer electrolyte. The discharge capacity at 333 K was reported to be about 100 mAh $g^{-1}$ with a discharge voltage plateau in both 4.7 and 4.1 V regions, while the cell without $Li_3PO_4$ showed a discharge plateau <3.5 V. In this report, we investigated the electrochemical stability of $LiMn_{1.5}Ni_{0.5}O_4$ cathode at room temperature and in the 5 V operational range. The improved electrochemical properties were explained on the basis of structural (XRD, micro-Raman spectroscopy), and microstructural (SEM, EDAX) results.

## 2. Experimental

Stoichiometric amounts of lithium acetate [$Li(CH_3COO)\cdot 2H_2O$], manganese(II) acetate [$Mn(CH_3COO)_2\cdot 4H_2O$] and nickel(II) acetate [$Ni(CH_3COO)_2\cdot 4H_2O$] were used as precursors (all taken from Alfa Aeser, 99.9% pure) and were separately dissolved in 2-ethylhexanoic acid with continuous stirring and slow heating. After half an hour, all solutions were mixed together followed by heating and continuous stirring up to boiling point for half an hour. The solution was allowed to evaporate at about 100 °C for 10 h, resulting in the formation of amorphous powders. The powder was again dried at 400 °C for 4 h. Finally, $LiMn_{1.5}Ni_{0.5}O_4$ phase was formed at a calcinations temperature of 850 °C for 14 h. The crystallinity of the powder was confirmed from the XRD pattern of the sample, using a Siemens D5000 X-ray powder diffractometer. The microstructure and compositions at various spots on the sample surface were analyzed using scanning electron microscope and energy-dispersive analysis by X-ray (JOEL, EDAX). The spinel structure (space group $Fd\bar{3}m$) was further verified from the micro-Raman spectroscopic measurements, carried out using a Jobin-Yvon T64000 spectrometer. The microstructures of the virgin and cycled cathode materials were taken from scanning electron microscope measurements. The electrochemical measurements (cyclic voltammetry and charge–discharge characteristics) were performed using a Gamry Instruments potentiostat and PHE200 electrochemical software.

The cathode was prepared by mixing calcined powder ($LiMn_{1.5}Ni_{0.5}O_4$), carbon black and polyvinylidene fluoride (weight ratio 80:10:10), and subsequently a slurry was made with *n*-methyl pyrolidone. The resulting paste was cast uniformly onto aluminum foil followed by drying at about 100 °C in an oven overnight. Li metal foil was used as the anode. Coin cells were prepared in an argon atmosphere inside a Glove Box (MBraun, USA). The cathode and Li anode were separated inside the coin cell using Celgard 2400 membrane. Lithium hexafluorophosphate, dissolved in mixture of ethylene carbonate (EC) and dimethyl carbonate (DMC) in (1:1, v/v) was used as electrolyte.

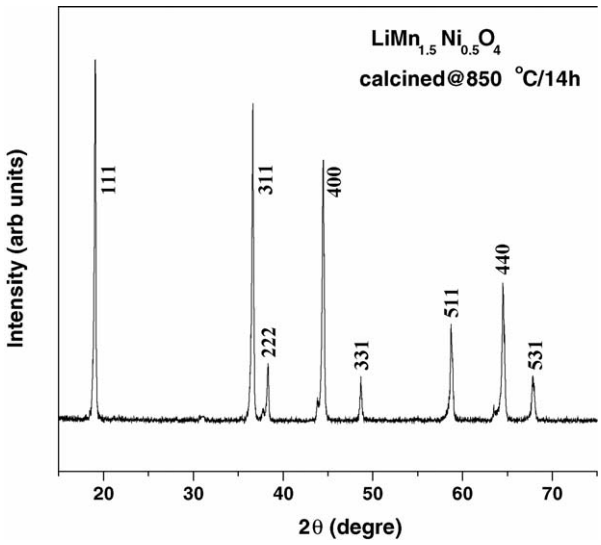


Fig. 1. XRD pattern of as-prepared $LiMn_{1.5}Ni_{0.5}O_4$ cathode calcined at 850 °C for 14 h.

## 3. Results and discussions

Fig. 1 shows the XRD pattern of as-prepared $LiMn_{1.5}Ni_{0.5}O_4$ cathode calcined at 850 °C for 14 h. It is evident that all the peaks present in the pattern correspond to the spinel structure of $LiMn_2O_4$, revealing the incorporation of Ni atoms onto the Mn sites. The absence of NiO, or any other lithium manganese oxide phase indicates that there is no segregation of unwanted phases. The sharp peaks in the pattern show good crystallinity of the cathode. We calculated the lattice constants of $LiMn_{1.5}Ni_{0.5}O_4$ cathode, using the Sherrer formula for cubic spinels and found it to be about 8.1809 Å, which is slightly less than that of a pure $LiMn_2O_4$ cathode material (8.248 Å) [21]. Fig. 2 shows the surface morphology of the cathode material before electrochemical cycling. As observed from the micrograph, there is a significant variation in the grain size, ranging from ~0.5 to ~4.0 μm in diameter. The grains were not uniformly distributed over the sample surface. We selected two different spots over the sample

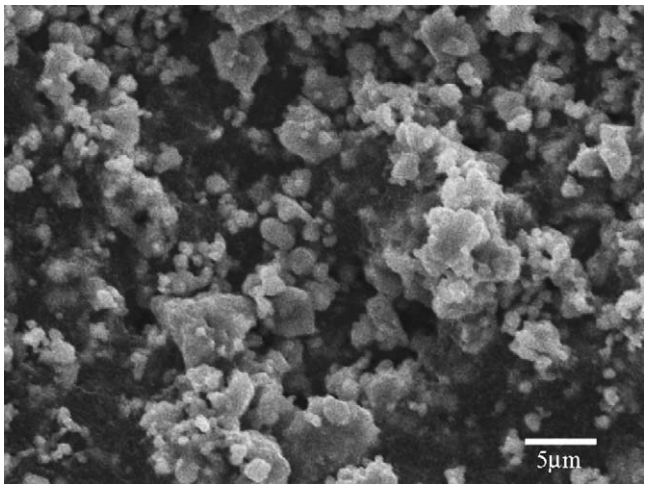


Fig. 2. SEM micrograph of as-prepared $LiMn_{1.5}Ni_{0.5}O_4$ cathode.

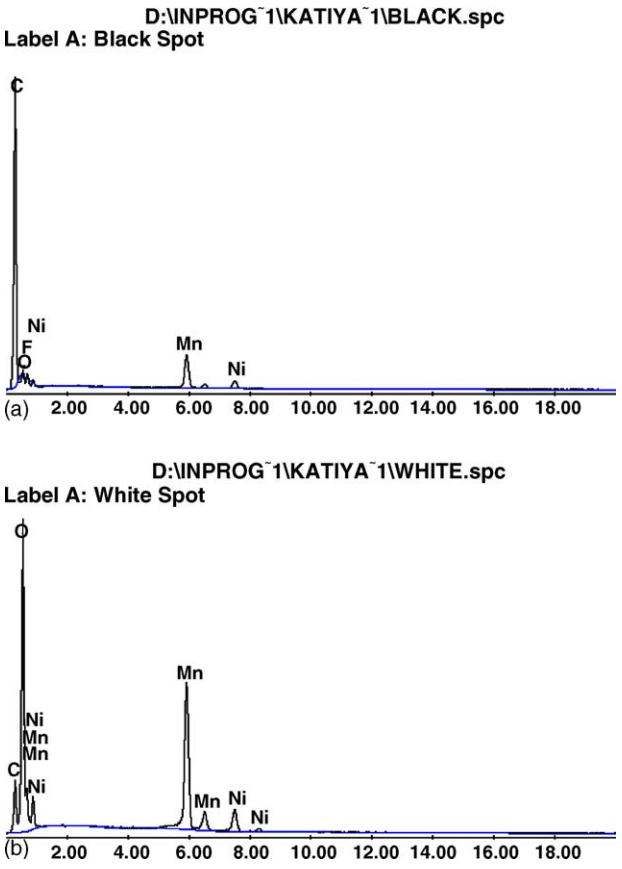


Fig. 3. Energy-dispersive analysis by X-ray taken (a) at a black spot on sample surface, (b) at a white spot on sample surface.

surface (one in the black area, and other in the white area of the SEM micrograph) to investigate the surface compositions, using energy-dispersive analysis by X-ray (EDAX). The spectrum is shown in Fig. 3a and b, respectively. The black area corresponds to carbon rich portion of the sample, originating from the carbon black used during the cathode preparation. The white area corresponds to the active material rich portion of the sample. So, we conclude that there are non-uniform distributions of $LiMn_{1.5}Ni_{0.5}O_4$ grains embedded in carbon black rich area inside the as-prepared cathode. It was reported by earlier workers that, pure $LiMn_2O_4$ has a cubic spinel structure having space group $Fd\,\bar{3}m$ [22]. According to the group theoretical calculations, there are five Raman active modes for $LiMn_2O_4$, one of $A_{1g}$ symmetry, one of $E_g$ symmetry, and three of $T_{2g}$ symmetry. The calculated positions of these modes by Ammundsen et al. [23] are at 598, 434, 354, 455, and 597 $cm^{-1}$, respectively. Fig. 4 shows the micro-Raman spectra of $LiMn_{1.5}Ni_{0.5}O_4$ for the as-prepared cathode. After fitting the data with the phonon function, we observed all five bands which corresponded to 615.06, 447.8, 364.11, 484.72 and 579.09 $cm^{-1}$ in the virgin cathode. We assigned these four bands as $A_{1g}$, $E_g$, and two $T_{2g}$ modes, respectively. However, these differ from the calculated values for $LiMn_2O_4$ because of the possible disorder in all the cations and oxygen anions in the lattice and also because of the difference in the Mn–O and Ni–O vibrations. The Mn, Ni ions are motionless in the $A_{1g}$ and $E_g$ phonon modes, involving only oxide ion

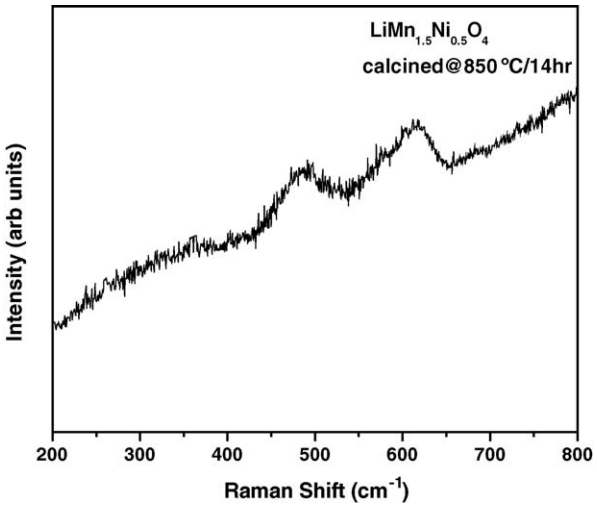


Fig. 4. Micro-Raman spectra of $LiMn_{1.5}Ni_{0.5}O_4$ as-prepared cathode, taken by a Jobin-Yvon T64000 spectrometer in backscattered geometry.

displacements, $T_{2g}$ phonons at 455 and 597 $cm^{-1}$ involve large oxygen motions and very small lithium displacements, and the $T_{2g}$ phonon at 354 $cm^{-1}$ originates from the vibration of the lithium sublattice.

Fig. 5 shows the cyclic voltammetry of the coin cell in 5 V range (voltage scan 3.5–5.3 V), measured at a scan rate of 0.1 mV $s^{-1}$. The voltagram clearly shows the oxidation and reduction peaks corresponding to spinel $LiMn_2O_4$ as well as $Ni^{2+}$ to $Ni^{4+}$ oxidation and reduction peaks. This evidence suggested that in addition to manganese oxidation and reduction, nickel can also be oxidized and reduced at higher voltage (4.862 and 5.05 V, respectively) in $LiMn_{1.5}Ni_{0.5}O_4$ and hence can be operated at 5 V range in a coin cell. Also, the higher intensity corresponding to nickel oxidation and reduction processes reveals its suitability for 5 V applications. However, we could not further resolve the progressive oxidations of $Ni^{2+}$ to $Ni^{3+}$ to $Ni^{4+}$ from the voltagram since the peaks at higher voltages merge

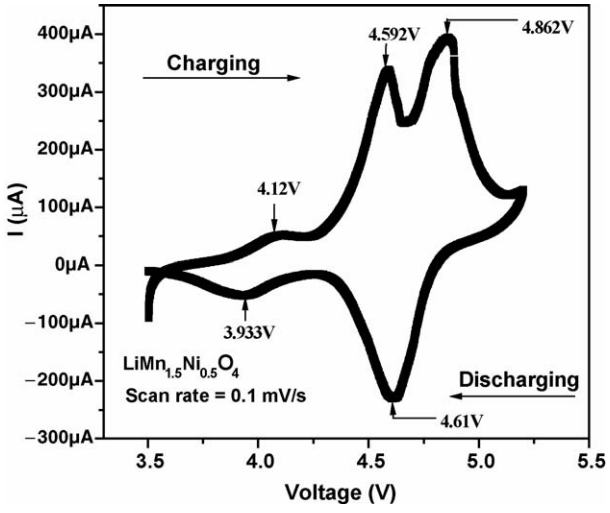


Fig. 5. Cyclic voltammetry of $LiMn_{1.5}Ni_{0.5}O_4$/(EC + DMC)/Li coin cell in 3.5–5.3 V range at scan rate of 0.1 mV $s^{-1}$.

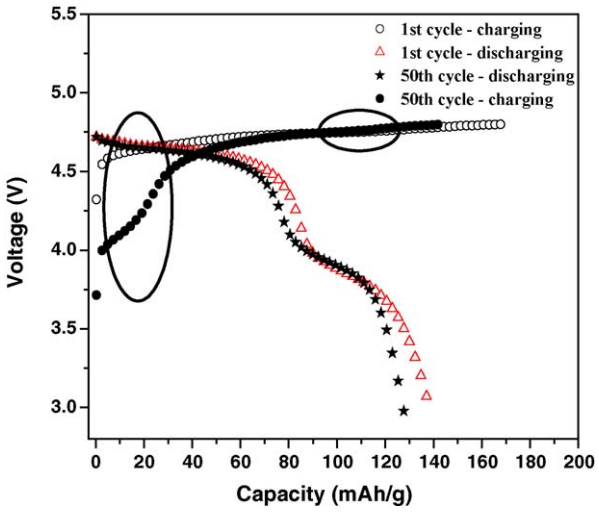


Fig. 6. Room temperature charge–discharge characteristics of first and 50th cycle of $LiMn_{1.5}Ni_{0.5}O_4$/(EC + DMC)/Li coin cell at 0.2 mA $cm^{-2}$ between 3.5 and 5.3 V.

together. The coulombic efficiency from the cyclic voltammetry was found to be about 93%.

Fig. 6 shows the room temperature charge–discharge characteristics of the coin cell performed galvanostatically at a load current of 0.2 mA $cm^{-2}$ between 3.0 and 4.8 V cut-off limits. In each cycle, the cell started charging from the open circuit voltage. The cell delivered an excellent initial specific discharge capacity of 140 mAh $g^{-1}$ with a very good cyclability for 50 cycles. The charge–discharge characteristics of both the first cycle and 50th cycle are compared in Fig. 6. Fig. 7 shows the cyclability plot and the percentage of initial discharge capacity retention after 50 cycles which was calculated to be 94%. The experimental capacity obtained is close to the theoretical capacity for $LiMn_{1.5}Ni_{0.5}O_4$, which is 146.6 mAh $g^{-1}$ (assuming all $Li^+$ ions inserted into $LiMn_{1.5}Ni_{0.5}O_4$). There are several potential plateaus observed in the charge–discharge characteristics. During charging, there are total three plateaus observed; one of them is around the 4 V range, which corresponds to the redox reaction involving $Mn^{3+}/Mn^{4+}$. Two more plateaus are observed in the 4.5–4.7 and 4.7–4.9 V potential regions. These two plateaus correspond to the redox reactions involving $Ni^{2+}/Ni^{3+}$ and $Ni^{3+}/Ni^{4+}$, respectively. During discharging, two plateaus were observed; one corresponds to reduction of $Ni^{4+}$ to $Ni^{2+}$ in the 5 V region, and the other corresponds to the reduction of $Mn^{4+}$ to $Mn^{3+}$ in the 4 V region. Correlating the cyclic voltammetry and charge–discharge characteristics reveals that the voltage plateaus observed in the latter exactly correspond to the anodic and cathodic peaks. The coulombic efficiencies for the first and 50th charge–discharge cycle were found to be about 83.33% and 90.34%, respectively.

In order to investigate the structural stability of $LiMn_{1.5}Ni_{0.5}O_4$ cathode and to correlate it into its electrochemical performances, we carried out XRD, SEM, and micro-Raman spectroscopic studies of the cycled sample. Fig. 8 compares the XRD plots of as prepared and the cycled cathode. All the spinel peaks are present in the spectrum indicating that the cathode still retained the spinel structure after 50 cycles of charging–discharging. Close observation reveals that all the peaks are slightly shifted towards lower values of the diffraction angle. We calculated the lattice parameters and found them to decrease from 8.1809 to 8.1632 Å. The crystallite size and lattice strain were calculated using the Williamson Hall Equation [24]. The crystallite size before and after cycling was found to be about 37.098 and 30.06 Å, respectively, while the lattice strain before and after cycling was found to be about 0.2977 and 0.1401, respectively. The decrease in crystallite size and lattice strain could be due to the slight decrease in the lattice constant of the spinel unit cell. Fig. 9 shows the SEM pictures of the cathode after 50 cycles of charging and discharging. The sample surface, grain size resemble with those before the electrochemical cycling. One of the degradation mechanisms in $LiMn_2O_4$ cathode materials is attributed to the formation of a solid electrolyte interface (SEI) layer on both the cathode and anode surface from several reports in the literature [25–28]. And also

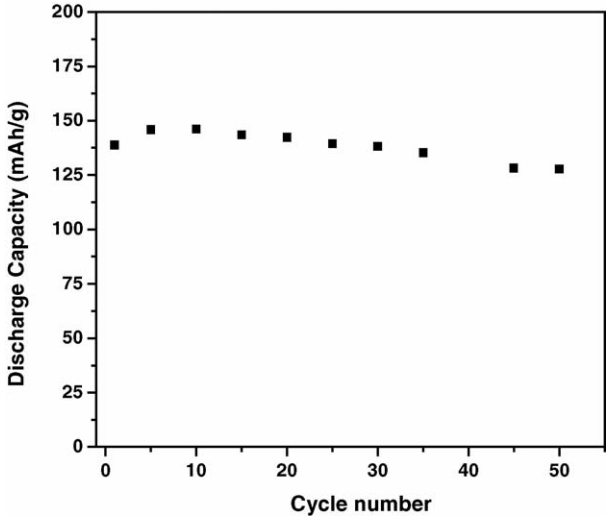


Fig. 7. The specific capacity vs. number of cycle of the $LiMn_{1.5}Ni_{0.5}O_4$/(EC + DMC)/Li coin cell.

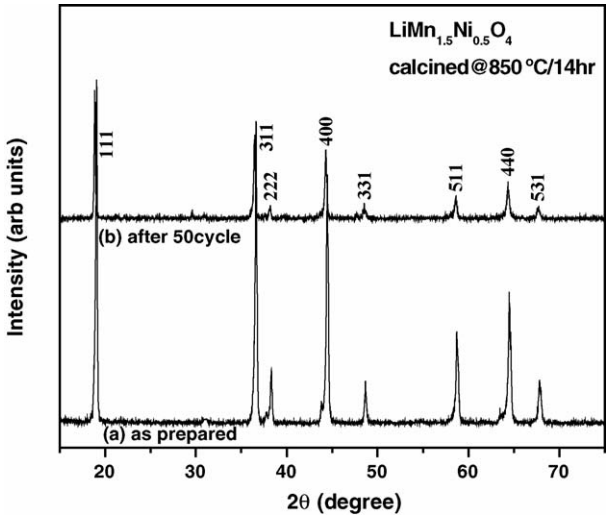


Fig. 8. Comparison of the XRD patterns of as prepared and 50 times electrochemically cycled $LiMn_{1.5}Ni_{0.5}O_4$.

Table 1
Comparison of Raman peak positions of $LiMn_{1.5}Ni_{0.5}O_4$ cathode before and after electrochemical cycling and with Raman peaks of pure $LiMn_2O_4$ Ref. [23]

| Phonon symmetry | $LiMn_2O_4$ (calculated position in $cm^{-1}$—Ref. [23]) | $LiMn_2O_4$ (observed position in $cm^{-1}$—Ref. [23]) | $LiMn_{1.5}Ni_{0.5}O_4$ (peak position in $cm^{-1}$ observed in this work—before electrochemical cycling) | $LiMn_{1.5}Ni_{0.5}O_4$ (peak position observed in this work—after 50 electrochemical cycling) | Shift in peak position after 50 cycles ($cm^{-1}$) |
|---|---|---|---|---|---|
| $A_{1g}$ | 598 | 625 | 615.06 | 587.16 | 27.9 |
| $E_g$ | 434 | 432 | 447.8 | 413.95 | 33.85 |
| $T_{2g}^{(1)}$ | 354 | 365 | 364.11 | 352.9 | 11.21 |
| $T_{2g}^{(2)}$ | 455 | 480 | 484.72 | 471.75 | 12.97 |
| $T_{2g}^{(3)}$ | 597 | 590 | 579.09 | 548.44 | 30.65 |

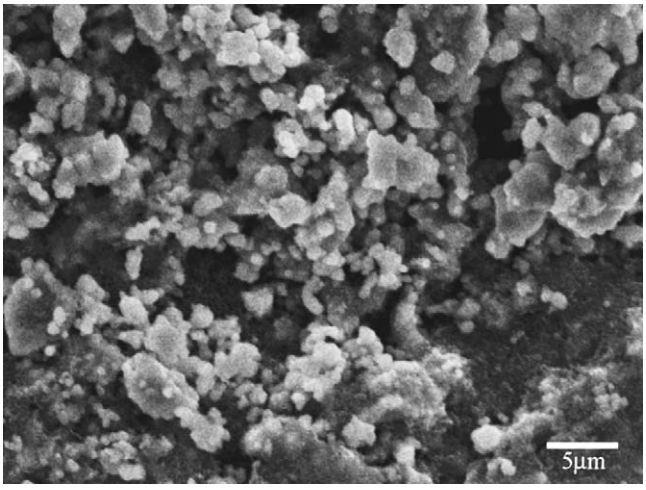


Fig. 9. SEM pictures of the cathode after 50 cycles of charging and discharging.

we have observed the formation of such a layer on the $LiMn_2O_4$ nanocrystalline thin film cathode [29]. However, in this work we believe that the bigger grain size and hence large surface area may be a reason to protect the formation of continuous electrochemical interfacial resistance layer to hinder the insertion and extraction of $Li^+$ ion. Fig. 10 compares the Raman spectra of the virgin and electrochemically cycled cathodes. We calculated

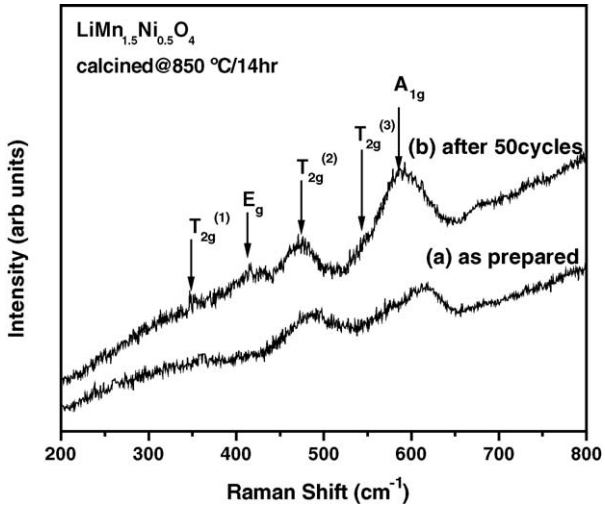


Fig. 10. Comparison of the Raman spectra of virgin and electrochemically cycled $LiMn_{1.5}Ni_{0.5}O_4$.

the shift in each of the Raman peaks using the phonon function, which is summarized in Table 1. All the phonon modes present in the virgin electrode were also present in the cycled electrode, but they were shifted towards lower wavelengths. The detailed study of the origin of the shifting in each of the peaks and its effect on the charge–discharge characteristics is in progress.

## 4. Conclusions

We have successfully synthesized a good quality $LiMn_{1.5}Ni_{0.5}O_4$ cathode by an acetate based chemical solution route after optimizing the process parameters. The spinel structure of the cathode was verified from the XRD and Raman spectroscopic measurements. Using this cathode, a Li anode and $LiPF_6$ dissolved in DMC + EC (1:1, v/v ratio) as the electrolyte, we fabricated coin cells and performed electrochemical tests. The presence of symmetry for all the redox peaks in the cyclic voltagram confirmed the reversible charge transport inside the cell. The higher voltage $Ni^{2+} \leftrightarrow Ni^{4+}$ redox peaks clearly demonstrated the possibility of using the cell in high voltage applications. The high coulombic density of the electrochemical cell was corroborated from the initial specific discharge capacity of 140 mAh $g^{-1}$ and the stability of the cell up to 50 repeated cycling with ~94% retention of initial discharge capacity. The electrochemical stability is in good agreement with the structural integrity, as supported by XRD, micro-Raman, and SEM measurements of the cathode after electrochemical cycling.

## Acknowledgements

The above research work was partially supported by the research grants from DoE (# DE-FG02-01ER45868) and NASA (#NAG3-2676) Glenn research center. The support from UPR Materials Characterization Center (MCC) is acknowledged.

## References

[1] K. Mizushima, P.C. Jones, P.J. Wiseman, J.B. Goodenough, Mater. Res. Bull. 15 (1980) 783.
[2] J.M. Tarascon, E. Wang, F.K. Shokoohi, W.R. McKinnon, S. Colson, J. Electrochem. Soc. 138 (1991) 2859.
[3] M.M. Thackeray, W.I.F. David, P.G. Bruce, J.B. Goodenough, Mater. Res. Bull. 18 (1983) 461.
[4] J.M. Tarascon, M. Armand, Nature 414 (2001) 359.
[5] Y.M. Chiang, D.R. Sadoway, Y.I. Jang, B. Huang, H. Wang, Electrochem. Solid-State Lett. 2 (1999) 107.

[6] G.G. Amatucci, J.M. Tarascon, L.C. Klein, J. Electrochem. Soc. 143 (1996) 1114.
[7] L. Croguennec, C. Pouillerie, C. Delmas, J. Electrochem. Soc. 147 (2000) 1314.
[8] J. Cho, M.M. Thackeray, J. Electrochem. Soc. 146 (1999) 3577.
[9] M.M. Thackrey, Y. Shao-Horn, A.J. Kahaian, K.D. Kepler, E. Skinner, J.T. Vaughey, S.A. Hackney, Electrochem. Solid-State Lett. 1 (1998) 7.
[10] H. Huang, C.H. Chen, R.C. Perego, E.M. Kelder, L. Chen, J. Schoonman, W.J. Weydanz, D.W. Nielsen, Solid State Ionics 127 (2000) 31.
[11] I. Tomeno, Y. Kasuya, Y. Tsunoda, PR B64 (2001) 094422.
[12] K.Y. Chung, K.-B. Kim, J. Electrochem. Soc. 149 (2002) A79.
[13] Y.-K. Sun, Y.-S. Jeon, H.J. Leeb, Electrochem. Solid-State Lett. 3 (2000) 7.
[14] G.G. Amatucci, N. Pereira, T. Zheng, J.-M. Tarascon, J. Electrochem. Soc. 148 (2001) A171.
[15] J. Cho, B. Park, Electrochem. Solid-State Lett. 3 (2000) 355.
[16] G. Ting-Kuo Fey, C.-Z. Lu, T. Prem Kumar, J. Power Sources 115 (2003) 332.
[17] S. Nieto, S.B. Majumder, R.S. Katiyar, J. Power Sources 136 (2004) 88.
[18] Y.K. Sun, Y.S. Lee, M. Yoshio, K. Amine, Electrochem. Solid-State Lett. 5 (2002) A99.
[19] K. Kanamura, W. Hoshikawa, T. Umegaki, J. Electrochem. Soc. 149 (2002) A339.
[20] Y. Kobayashi, H. Miyashiro, K. Takei, H. Shigemura, M. Tabuchi, H. Kageyama, T. Iwahori, J. Electrochem. Soc. 150 (2003) A1586.
[21] S.H. Kang, J.B. Goodenough, J. Electrochem. Soc. 147 (2000) 3621.
[22] M.M. Thackeray, Prog. Solid State Chem. 25 (1997) 1.
[23] B. Ammundsen, G.R. Burns, M.S. Islam, H. Kanoh, J. Roziere, J. Phys. Chem. B103 (1999) 5175.
[24] G.K. Williamson, W.H. Hall, Acta Metall. 1 (1953) 222.
[25] D. Aurbach, M.D. Levi, E. Levi, H. Teller, B. Markovsky, G. Salitra, J. Electrochem Soc. 145 (1998) 3024.
[26] Y. Matsuo, R. Kosteeki, F. MeLarnon, J. Electrochem. Soc. 148 (2001) A687.
[27] S.S. Zhang, K. Xu, T.R. Jow, J. Electrochem. Soc. 149 (2002) A1521.
[28] S. Zhang, M.S. Ding, K. Xu, J. Allen, T.R. Jow, Electrochem. Solid-State Lett. 4 (2001) A206.
[29] S.R. Das, S.B. Majumder, R.S. Katiyar, J. Power Sources 139 (2005) 261.